Magnetic field and pressure phase diagrams of the triangular-lattice antiferromagnet CsCuCl 3 explored via magnetic susceptibility measurements with a proximity-detector oscillator

K. Nihongi, T. Kida, Y. Narumi, Julien Zaccaro, Y. Kousaka, K. Inoue, K. Kindo, Y. Uwatoko, M. Hagiwara

HAL Id: hal-03740294
https://hal.science/hal-03740294

Submitted on 16 Aug 2022

Magnetic-field and pressure phase diagram of the triangular lattice antiferromagnet CsCuCl$_3$ clarified by magnetic susceptibility measured with a proximity detector oscillator

K. Nihongi,[1] T. Kida,[1] Y. Narumi,[1] J. Zaccaro,[2] Y. Kousaka,[3]

K. Inoue,[4,5] K. Kindo,[6] Y. Uwatoko,[6] and M. Hagiwara[1,5,*]

[1]*Center for Advanced High Magnetic Field Science (AHMF),*

Graduate School of Science, Osaka University, Toyonaka, Osaka 560-0043, Japan

[2]*Grenoble Alpes University, CNRS, Grenoble INP,*

Institut Néel, 38042 Grenoble, France

[3]*Department of Physics and Electronics,*

Osaka Prefecture University, Sakai, Osaka 599-8531, Japan

[4]*Graduate School of Science, Hiroshima University, Hiroshima 739-8526, Japan*

[5]*Center for Chiral Science, Hiroshima University, Hiroshima 739-8526, Japan*

[6]*The Institute for Solid State Physics,*

The University of Tokyo, Kashiwa, Chiba 277-8581, Japan

(Dated: March 15, 2022)

Abstract

The effect of pressure (P) on magnetic susceptibility of CsCuCl$_3$ was examined in magnetic fields ($\mu_0 H$) of up to 51 T using a proximity detector oscillator (PDO), and the H-P phase diagram of CsCuCl$_3$ was constructed over the saturation field (H_{sat}). We found that, with increasing P, H_{sat} increases and the uud-phase that appeared at $P = 0.7$ GPa widened. Based on comparison between the experimental and calculated H-P phase diagrams, the Y-phase was predicted to appear above 1.7 GPa. The interchain antiferromagnetic exchange interaction in the ab-plane was evaluated and found to increase with increasing P, which is consistent with a previous study under high pressure [D. Yamamoto *et al.*, Nat. Commun. **12**, 4263 (2021).]. Moreover, an anomaly was observed below $P = 0.6$ GPa just below H_{sat} and might be a new phase transition derived from nonlinear response caused by the PDO technique.

INTRODUCTION

Geometrically frustrated magnets have been studied over the past several decades owing to a rich variety of exotic physical phenomena [1, 2]. One of the most typical geometrically frustrated magnets is the two-dimensional triangular lattice antiferromagnet (TLA) [3]. The ground state infinitely degenerates in magnetic fields, and a small perturbation, such as easy-plane anisotropy, lifts the degeneracy and stabilizes the one-energy state [4], for example, an umbrella spin structure in low-magnetic fields normal to the easy plane. For classical spin systems, extensive theoretical studies have been conducted [5–7], and one of the experimental realizations is $RbFe(MoO_4)_2$ [8, 9]. When spins are small, quantum fluctuations play an important role in lifting degeneracy in some cases. For TLAs, the up-up-down (uud) state, which corresponds to a magnetization plateau at one-third of the saturation magnetization, is an exotic ground state [5–7, 10, 11] caused by the order-by-disorder mechanism [12] in magnetic fields. To date, Cs_2CuBr_4 [13–15] (not equilateral) and $Ba_3CoSb_2O_9$ [16, 17] are known to exhibit the uud ground state of $S = 1/2$ TLAs in magnetic fields.

$CsCuCl_3$ has been studied for a long time as one of ABX_3 compounds [18]. It is a TLA compound formed by ferromagnetic chains and exhibits a quantum phase transition in magnetic fields [19, 20]. The crystal structure of $CsCuCl_3$ at room temperature is hexagonal with a space group $P6_122$ or $P6_522$ [21, 22]. Magnetic Cu^{2+} ions of $CsCuCl_3$ with $S = 1/2$ form a helical chain structure with a sixfold periodicity along the c-direction and triangular lattices in the ab-plane. The spin Hamiltonian for $CsCuCl_3$ in magnetic fields [20] is given by,

$$\mathcal{H} = - 2J_0 \sum_{i,n} (S_{i,n} \cdot S_{i,n+1} + \eta(S_{i,n}^x S_{i,n+1}^x + S_{i,n}^y S_{i,n+1}^y))$$
$$+ 2J_1 \sum_{<i,j>,n} (S_{i,n} \cdot S_{i,n+1}) - \sum_{i,n} D_{n,n+1} \cdot (S_{i,n} \times S_{i,n+1})$$
$$- g\mu_B H \sum_{i,n} S_{i,n}^z, \tag{1}$$

where $S_{i,n}$ represents a spin located at the i-th site in the n-th ab-plane, and the summation $\langle ij \rangle_n$ is taken over all nearest-neighbor pairs in the n-th ab-plane. The z-axis is assumed to be parallel to the c-axis. The first and second terms are the intrachain ferromagnetic exchange (exchange constant $J_0 > 0$) and interchain antiferromagnetic exchange (exchange constant $J_1 > 0$) interactions, respectively. $\eta (> 0)$ represent a weak anisotropic exchange ratio for the easy plane. The

third term represents the Dzyaloshinskii-Moriya (DM) interaction where $\boldsymbol{D}_{n,n+1}$ represents the DM vector between adjacent spins in the n-th and $(n+1)$-th c-planes. The fourth term is the Zeeman energy. g and μ_B are the g-factors for the z-axis and Bohr magneton, respectively.

The intrachain and interchain exchange constants were evaluated based on the following analyses: $J_0/k_B = 24 \pm 3$ K and $J_1/k_B = 3.8 \pm 1$ K from magnetic susceptibilities [23], $J_0/k_B = 28$ K and $J_1/k_B = 4.9$ K from electron spin resonance (ESR) excitation modes for $H \parallel c$ [24], and $J_0/k_B = 28$ K (2.4 meV) and $J_1/k_B = 4.6$ K (0.4 meV) from inelastic neutron scattering data [25]. The Cu spins exhibited a 120° spin structure in the ab-plane below the Néel temperature $T_N = 10.7$ K [26, 27]. The Cu chain structure along the c-axis allows DM interaction with a uniform $\boldsymbol{D}$ vector pointing in the chain direction ($D/k_B = 5.1$ K [24] or 5.8 K [25]) owing to the chiral crystal structure [26, 28]. Below T_N, the nearest-neighbor spins along the c-axis were rotated with a pitch angle of $\theta = 5.1 \pm 0.1°$ in the ab-plane [26]. In the following analysis of our experimental data, we used the parameter values obtained by the analysis of ESR excitation modes [24]: $J_0/k_B = 28$ K and $J_1/k_B = 4.9$ K, and $D/k_B = 5.1$ K .

The magnetization (M) of CsCuCl$_3$ for $H \parallel c$ at 1.1 K increased almost linearly and showed a jump at 12.5 T, then increased again and saturated at 31 T [19]. Nikuni and Shiba interpreted the magnetization process of CsCuCl$_3$ for $H \parallel c$ [20] using the spin Hamiltonian (Eq.(1)). They eliminated the asymmetric part from the Hamiltonian by rotating the xy-plane with pitch $q = \tan^{-1}(D/2J_0 (1 + \eta))$. Thereafter, the spin Hamiltonian can be simply rewritten as:

$$\mathcal{H} = -\sum_{i,n}[2\tilde{J}_0(S^x_{i,n}S^x_{i,n+1} + S^y_{i,n}S^y_{i,n+1}) + 2J_0 S^z_{in}S^z_{in+1}]$$
$$+ 2J_1 \sum_{<ij>n} \boldsymbol{S}_{in} \cdot \boldsymbol{S}_{jn} - g\mu_B H \sum_{i,n} S^z_{i,n}, \tag{2}$$

where $\tilde{J}_0 = J_0 \sqrt{(1 + \eta)^2 + (D/2J_0)^2}$. They defined the easy-plane anisotropy as,

$$\Delta \equiv (\tilde{J}_0 - J_0)/J_1. \tag{3}$$

Thereafter, the value of saturation field is given by,

$$H_{sat} = (18 + 4\Delta)J_1 S/g\mu_B. \tag{4}$$

They interpreted that the jump in M of CsCuCl$_3$ for $H \parallel c$ was caused by the quantum phase

transition from the umbrella to 2-1 coplanar phase. Their theoretical predictions were confirmed by neutron diffraction [29] in magnetic fields.

The application of high pressure is a powerful method that can alter the magnetic properties of a material by shrinking its crystal lattice. As for TLAs, magnetic anisotropy and the exchange interaction between magnetic ions vary through the change in distance and angle between the neighboring magnetic ions through intervening nonmagnetic ions by applying pressure. For the anisotropic TLA Cs_2CuCl_4, the appearance of a number of field-induced magnetic phase transitions upon pressure application have been reported, accompanied by an increase in the exchange coupling ratio J'/J, where J and J' are the exchange interactions on the horizontal and diagonal bonds in the spatially anisotropic triangular lattice, respectively [30].

Sera $et\ al.$ [31] performed magnetization measurements of $CsCuCl_3$ at 1.4 K in magnetic fields (μ_0H up to 15 T) along the c-axis under high pressure (P up to 0.9 GPa) and observed the magnetization plateau with $0.34\,\mu_B/Cu^{2+}$ under $P \geq 0.68$ GPa, which corresponds to the uud phase in M. Hosoi $et\ al.$ tried to explain the magnetization under high pressure by assuming that Δ was sensitive to pressure [32]. They constructed the magnetic phase diagram of $CsCuCl_3$ at 0 K under pressure by calculating the spin Hamiltonian based on spin-wave theory with Δ ($\Delta = 0.07$ at ambient pressure) as a variable of pressure. Δ decreased with increasing pressure, and the uud and Y coplanar phases under high pressure ($\Delta \leq 0.06$) were predicted to appear with the fixed parameters of J_0 and $\tilde{J}_0$. Yamamoto $et\ al.$ demonstrated theoretically that the ratio of J_0 to J_1 reduces with pressure, and then the uud and Y coplanar phases appeared under $P \geq 0.75$ GPa, corresponding to the results of magnetic measurement of $CsCuCl_3$ under high pressure up to 1.21 GPa in magnetic fields of up to 5 T [33]. In both theories, the change in the ratio of J_0 to J_1 was important for the appearance of the field- and pressure-induced magnetic phases. A quantitative comparison of the H-P phase diagram of $CsCuCl_3$ requires J_1 under high pressure which was directly estimated from H_{sat}. Therefore, in this study, we investigated the pressure dependence of the entire magnetization process of $CsCuCl_3$ over the saturation field using a proximity detector oscillator (PDO) system.

The remainder of this study is organized as follows. In Section 2, the sample preparation of single crystals of $CsCuCl_3$, experimental methods and conditions are described. The experimental results of the pressure dependence of magnetic susceptibility up to 1.72 GPa and the magnetic-field (H) versus pressure (P) phase diagram obtained experimentally are presented in Section 3. In Section 4, the constructed H-P phase diagram is compared with the calculated phase diagram by

4

Hosoi *et al.* [32]. The similarities and differences between them are discussed. Finally, the origin of the anomaly observed immediately below the saturation field in the *c*-direction is discussed, followed by a summary of this study.

EXPERIMENTAL

Single crystals of $CsCuCl_3$ were grown by evaporating an aqueous solution containing equimolar amounts of $CsCl$ and $CuCl_2 \cdot 2H_2O$. Pulsed magnetic fields of up to 51 T with a pulse duration of 35 ms were generated using a nondestructive pulse magnet at AHMF at Osaka University. High-field magnetization measurements were performed using an induction method with a pick-up coil at temperatures down to 1.4 K at ambient pressure. A PDO system [34] was utilized to measure the change in the PDO resonance frequency (Δf), which corresponded to the field change of the magnetization ($\Delta M/\Delta H$), namely magnetic susceptibility, in a magnetic insulator, as explained below, under high pressures of up to 1.72 GPa. When the magnetic insulator was placed inside the sensor coil of the LC tank circuit, the change in Δf in the magnetic field was proportional to $\Delta M/\Delta H$ [35]. In this study, we used a NiCrAl piston cylinder-type pressure cell (PCC) with the inner and outer diameters of 2.0 and 8.6 mm, respectively, and the pressure medium Daphne 7373 oil (Idemitsu Kosan Co.,Ltd.). The pressure in the sample space was calibrated using the change in the superconducting transition temperature of Sn [36]. A large field sweep rate of pulsed magnetic fields induced the Joule heating caused by eddy currents generated in a conducting material. Based on our preliminary experiments, we found that the temperature in the sample space changed slightly until approximately 6.5 ms (approximately 40 T in the ascending process when the maximum field was 51 T) from the start of magnetic-field generation.

EXPERIMENTAL RESULTS

Figure 1(a) shows the magnetization (M) and its field derivative (dM/dH) of $CsCuCl_3$ for $H \parallel c$ at 1.4 K under ambient pressure. A small jump at $H_{c1} = 12.5$ T in M, which corresponds to a peak in dM/dH, indicates the phase transition from the umbrella to 2-1 coplanar phase. A small hysteresis in M and dM/dH was observed around H_{c1}, indicating a first-order phase transition, and M was saturated at $H_{sat} = 30.2$ T. These features were consistent with those in a previous study [19]. Figure 1(b) shows the change in PDO resonance frequency versus the applied field (Δf_{sub}-H
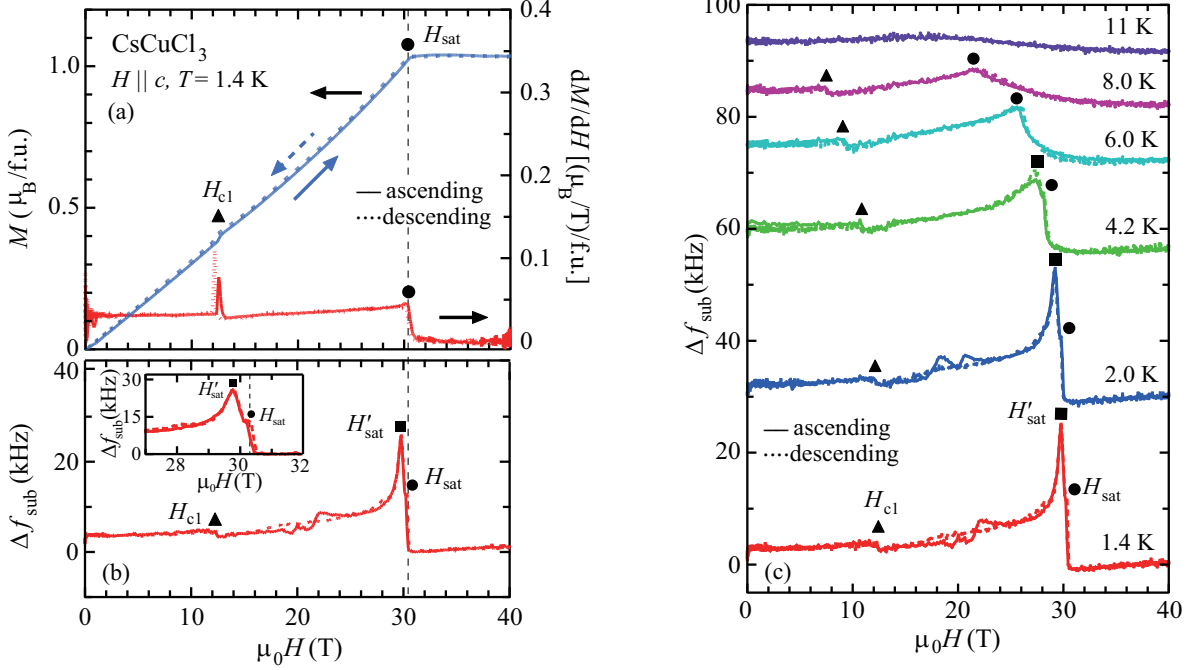
5

FIG. 1. (a) Magnetization (M) and dM/dH curves at 1.4 K observed in CsCuCl$_3$ for H parallel to the c-axis. The change in resonance frequencies (Δf_{sub}) against applied magnetic field for the c-axis of CsCuCl$_3$ at (b) 1.4 K and (c) various temperatures. Δf_{sub} is the frequency difference obtained by subtracting the frequency at T = 20 K as background from that at the measurement temperature. (In (a)-(c), solid and dotted lines are field ascending and descending processes, respectively.)

) curves of CsCuCl$_3$ for $H \parallel c$ at 1.4 K under ambient pressure. The Δf_{sub} value was obtained by subtracting the PDO frequency at T = 20 K as the background from that at each temperature. The Δf_{sub}-H curve at 1.4 K under ambient pressure indicates shoulders at H_{c1} and H_{sat}, and a sharp peak at H'_{sat} = 29.8 T, just below H_{sat} (Fig.1 (b) inset). An anomaly between 18 and 24 T in the field-ascending process was observed below 4.2 K, when the applied magnetic field went beyond H_{c1}, but the field range of the anomaly depends on the maximum applied field. The reason for this observation is currently unclear. The temperature dependence of the Δf_{sub}-H curve under ambient pressure is shown in Fig.1 (c). The shoulder at H_{c1} shifted to a lower field with increasing temperature and disappeared above T_N (=10.7 K). With increasing temperature, the shoulder at H_{sat} and the sharp peak at H'_{sat} shifted together to a lower magnetic field, merged above 6.0 K and disappeared above T_N. H'_{sat} may appear because of a magnetic phase transition caused by the AC response (MHz region) in the PDO measurements. In comparison, pulsed-field magnetization measurement was the low-frequency AC response at approximately 25 Hz and no sharp peak at

6

H'_{sat} in dM/dH was observed with the conventional method.

In the M and dM/dH curves for $H \perp c$ at 1.4 K under ambient pressure (Fig. 2 (a)), a plateau-like anomaly in M, which corresponds to a dip in dM/dH, was observed between 10 and 14 T, and the M was saturated at $H_{\text{sat}} = 29.3$ T. Figure 2(b) exhibits the Δf_{sub}-H curve for $H \perp c$ at 1.4 K under ambient pressure. A dip between 10 and 14 T and a peak at H_{sat} were observed. The sharp peak just below H_{sat} seen in the Δf_{sub}-H curves for $H \parallel c$ was not observed in the Δf_{sub}-H curve for $H \perp c$.

The pressure dependence of the Δf_{sub}-H curves of CsCuCl$_3$ for $H \parallel c$ at 1.4 K is shown in Fig. 3. The position of H_{c1} did not change significantly under $P < 0.90$ GPa. However, the shoulder at H_{c1} changed its structure to a dip with two shoulders when $P \geq 0.90$ GPa. We define the low and high transition fields as H_{c1} and H_{c2}, respectively. H_{c1} was nearly constant with increasing pressure even above 0.90 GPa. Contrarily, H_{c2} shifted to a higher magnetic field with increasing pressure above 0.90 GPa. The dip between H_{c1} and H_{c2} is suggested to be the uud phase reported in a previous study [19]. The anomaly between 18 and 24 T at ambient pressure shifted to a lower magnetic field with increasing pressure and disappeared under $P \geq 0.62$ GPa. The H'_{sat} and H_{sat} shifted together to a higher magnetic field with increasing pressure, and merged into one peak or broaden to form one peak at $P \geq 0.90$ GPa. The increase in H_{sat} indicates an increase in the
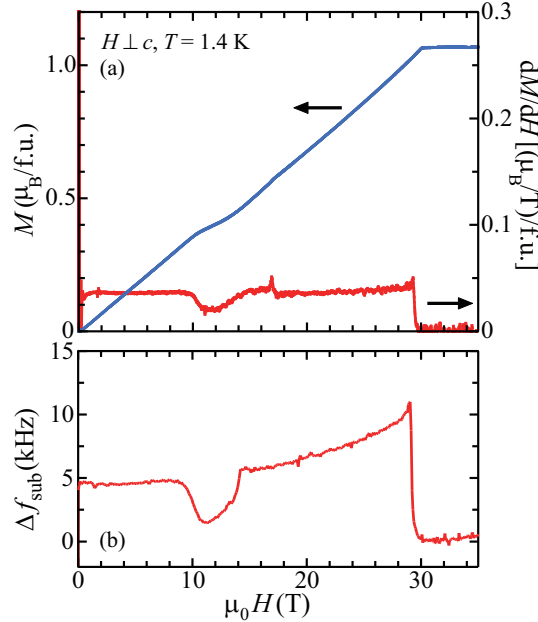

FIG. 2. (a) M (H) and dM/dH curves for $H \perp c$ at 1.4 K. (b) The change in resonance frequency (Δf_{sub}) for $H \perp c$ at 1.4 K. Δf_{sub} is the same definition as in the caption of Fig. 1.
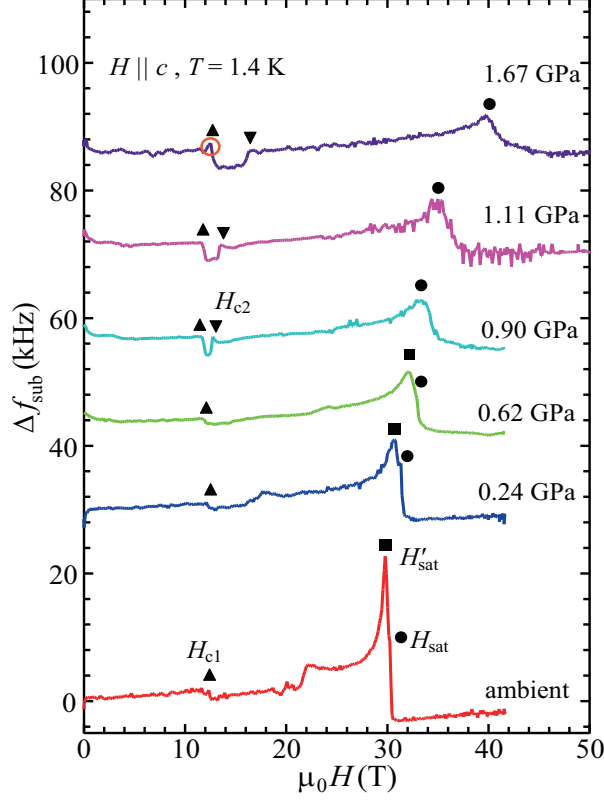
FIG. 3. Changes in resonance frequencies Δf_{sub}) of CsCuCl$_3$ for $H \parallel c$ at indicated pressures at 1.4 K. Δf_{sub} is the same definition as in the caption of Fig. 1. Each datum was taken from the field ascending process and shifts arbitrarily making it easier to see except for the ambient data. The small red circle at 1.67 GPa near H_{c1} is an anomaly which may correspond to the transition to the Y-phase. The data at ambient pressure were taken without pressure cell.

antiferromagnetic interaction in the *ab*-plane of CsCuCl$_3$, which may be caused by the shrinkage of the lattice in the *ab*-plane of CsCuCl$_3$ under pressure [37].

The magnetic field ($\mu_0 H$) versus the pressure phase diagram of CsCuCl$_3$ for $H \parallel c$ at 1.4 K is shown in Fig. 4. The pressure dependence of H_{sat} is well-fitted by the equation $H_{sat} = 30.2 + 2.14P + 2.14P^2$. H_{sat} is mainly determined by the antiferromagnetic exchange interaction in the *ab*-plane, as shown in Eq. (4). The field range of the uud phase between H_{c1} and H_{c2} expanded to a high-magnetic-field side with increasing pressure. The dashed lines extrapolated to the lower side from H_{c1} and H_{c2} intersect at approximately 0.7 GPa, which is in good agreement with the appearance of a magnetic plateau in M above 0.68 GPa in statice fields observed by Sera *et al.* [31]. The green magnetic phase near the saturation field in Fig. 4 is discussed in the next section.
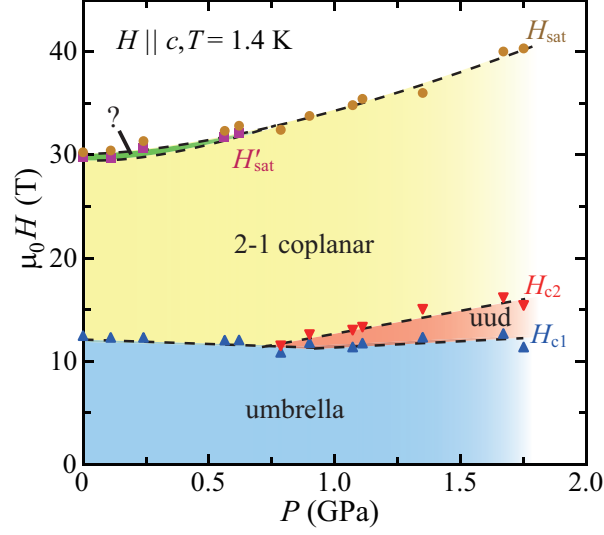
8

FIG. 4. Magnetic field ($\mu_0 H$) versus pressure (P) phase diagram of CsCuCl$_3$ for $H \parallel c$ at 1.4 K constructed by the PDO measurements.

DISCUSSION

Magnetic field ($\mu_0 H$) vs. pressure (P) phase diagram

We determined the interchain exchange constant J_1 and anisotropy parameter Δ from Eqs. (3) and (4), where the ferromagnetic intrachain exchange constant $J_0/k_B = 28$ K and $\tilde{J}_0 = 1.012\,J_0$
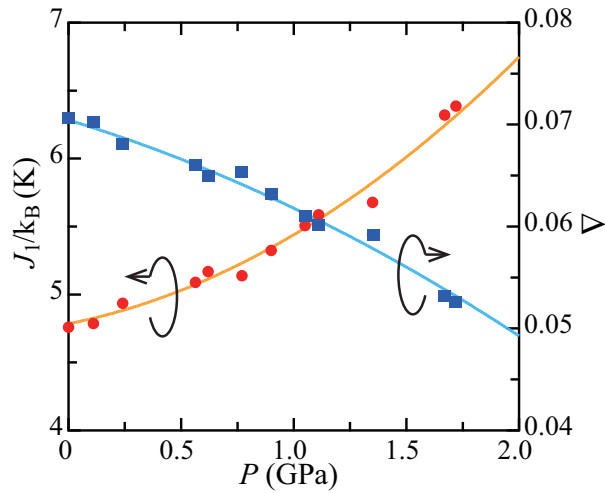

FIG. 5. Pressure (P) dependence of the interchain (in-plane) exchange constant J_1 and the anisotropy parameter Δ, when the intrachain exchange constant J_0 is assumed to be constant under high pressure.
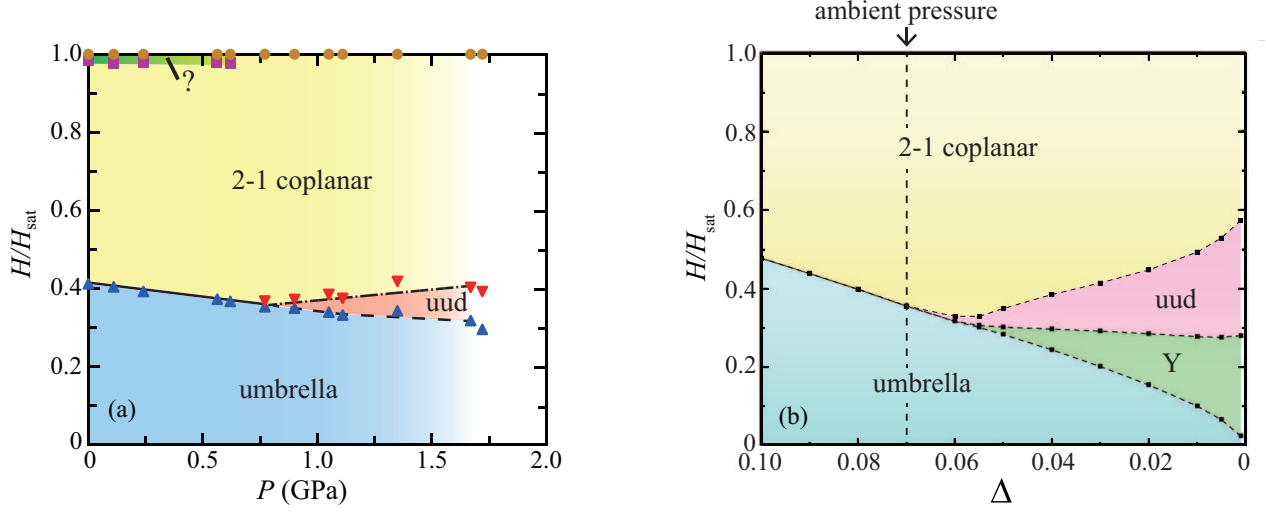
9

FIG. 6. (a) H/H_{sat} versus P phase diagram of $CsCuCl_3$ for $H \parallel c$ at 1.4 K. Solid, broken, and dot-dashed lines are the phase boundary between the umbrella and 2-1 coplanar phases, between the umbrella and uud phases, and between the uud and 2-1 coplanar phases, respectively. (b) Calculated H/H_{sat} versus Δ phase diagram constructed by reversing the horizontal axis from the phase diagram in Ref. [31]. The smaller Δ means the higher P, and $\Delta = 0.07$ corresponds to ambient pressure. By comparison, $\Delta = 0.055$ may correspond to $P \sim 1.7$ GPa.

were fixed under pressure, and J_1 (> 0) is the interchain antiferromagnetic exchange constant, as defined in the introduction. Figure 5 shows the pressure dependence of J_1 and Δ. The interchain exchange constant ($J_1/k_B = 4.8$ K at ambient pressure) was obtained from the saturation field, which is almost the same as that in Ref. [24]. J_1 increased with increasing pressure, whereas Δ decreased. The J_1/k_B and Δ were evaluated to be 6.4 K and 0.053 under the maximum pressure $P = 1.72$ GPa, respectively. In the pressure range of this study, Δ decreased from 0.070 to 0.053 ($4\Delta \ll 18$). J_1 depended strongly on H_{sat}, as shown in Eq. (4), because the change in Δ under pressure was quite small. Therefore, the pressure dependence of J_1 did not change much in both cases of J_0/k_B = constant and $J_0/k_B = 28.45 - 10.49P$ reported in Ref. [33] . The magnetic-field normalized by the H_{sat} versus pressure phase diagram of $CsCuCl_3$ is shown in Fig. 6(a). The similar calculated phase diagram by Hosoi *et al.* [32] is depicted in Fig. 6(b).The pressure dependences of H_{c1}/H_{sat} and H_{c2}/H_{sat} qualitatively agree with the calculation [32], and similar results were obtained by Yamamoto *et al.* [33]. The emergence of the Y coplanar phase was expected at $\Delta \leq 0.05$ and $H_{c1}/H_{sat} \leq 0.3$, as shown in Fig. 6 (b). In the Δf_{sub}-H curves for $H \parallel c$ at 1.4 K under $P = 1.67$ GPa, a small peak indicated by a red circle at H_{c1} corresponds to the
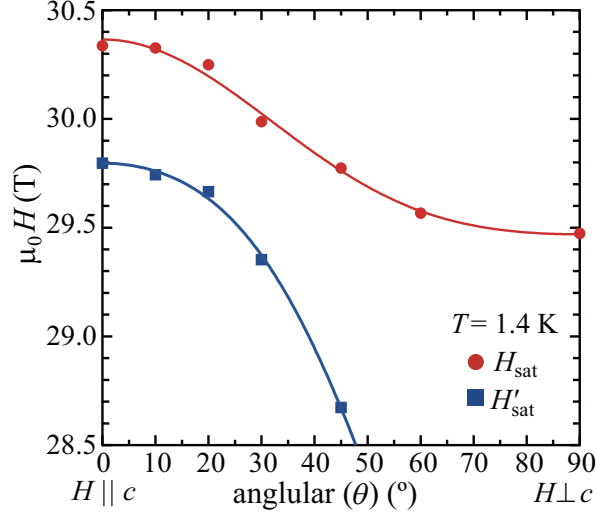
FIG. 7. Angular (θ) dependence of H'_{sat} and H_{sat} of $CsCuCl_3$ at 1.4 K. The solid lines are the fitting curves of H_{sat} and H'_{sat} with $H_{sat} = A\cos2\theta + B\cos4\theta + C$ and $H'_{sat} = A'\cos2\theta + B'\cos4\theta + C'$ (A, B, C, A', B', and C' are fitting parameters).

transition field from the umbrella to predicted Y coplanar phase [32]. The Y phase was expected to appear below $H_{c1}/H_{sat} = 0.3$ in Ref. [32] (Fig. 6 (b)), but the experimentally observed H_{c1}/H_{sat} was approximately 0.3 at the maximum pressure in this study. Therefore, we plan to perform PDO measurements at pressures above 1.72 GPa. A crystal structural phase transition in $CsCuCl_3$, however, was predicted at pressures between 1.65 and 3.1 GPa [37], and this transition may hinder the appearance of the Y-phase.

The anomaly just below the saturation field

The peak at H'_{sat} observed in the Δf_{sub}-H curve for $H \parallel c$ did not appear in the case of $H \perp c$. The angular dependences of H_{sat} and H'_{sat} are shown in Fig. 7, where θ is the angle between the applied magnetic field and c-axis. H_{sat} shifted gradually to a lower magnetic field with increasing. θ, but H'_{sat} shifted abruptly to a lower magnetic field with increasing θ until $\theta = 45°$, and then disappeared at $\theta > 45°$. The angle dependences of H_{sat} and H'_{sat} were fitted by the equations $H_{sat} = A\cos2\theta + B\cos4\theta + C$ and $H'_{sat} = A'\cos2\theta + B'\cos4\theta + C'$ (A, B, C, A', B' and C' are fitting parameters). The following parameter values were obtained from the fittings: $A = 0.448$, $B = 0.078$, $C = 29.8$, $A' = 1.69$, $B' = -0.280$, and $C' = 28.4$. In both cases, the coefficients of $\cos2\theta$ were dominant, although their magnitudes were largely different.

11

In the dM/dH curve of the triangular lattice antiferromagnet $NiBr_2$[38], a sharp peak, which corresponds to the antiferro-fan transition, was observed just below the saturation field. If the peak at H'_{sat} indicates a magnetic transition from the 2-1 coplanar to fan phase, it should be observed in conventional magnetization measurements of $CsCuCl_3$. However, no anomaly at H'_{sat} was observed in the M and dM/dH curves (Fig. 1(a)).

Why was the H'_{sat} anomaly observed in the PDO measurements? In the PDO measurements, $\Delta M/\Delta H$ in the insulating sample $CsCuCl_3$ was taken as Δf in high-frequency response (of the order of ten mega-hertz). The high-frequency response in magnetic fields may give rise to a nonlinear magnetic response owing to the third-harmonic component of χ_3 in the AC magnetic susceptibility measurements (M in the AC magnetic measurements is given by $M(H) = M_0 + \chi_1 H + \chi_3 H^3 + \cdot\cdot$). To clarify this interpretation, AC magnetic susceptibility measurements of $CsCuCl_3$ in high magnetic fields are required.

SUMMARY

We experimentally performed magnetic measurements of single-crystal samples of $CsCuCl_3$ in pulsed-high magnetic fields under high pressure using the PDO technique. We succeeded in measuring the shift of the PDO frequency that corresponds to the field derivation of magnetization over the saturation field, and clarified the pressure dependence of J_0 and Δ. The magnetic field versus pressure phase diagram of $CsCuCl_3$ constructed from the experimental results agrees qualitatively with that obtained by theoretical calculations [32, 33].The anomaly just below the saturation field for $H \parallel c$ at 1.4 - 4.2 K was observed in the PDO measurements and not in the conventional magnetization measurements. This anomaly may correspond to the transition field caused by the nonlinear AC magnetic response in PDO measurements.

* Corresponding author

[1] P. W. Anderson, Materials Research Bulletin **8**, 153 (1973).

[2] L. Balents, Nature **464**, 199 (2010).

[3] O. A. Starykh, Rep. Prog. Phys. **78**, 052502 (2015).

[4] D. Yamamoto, G. Marmorini, and I. Danshita, Phys. Rev. Lett. **112**, 127203 (2014).

[5] H. Kawamura and S. Miyashita, J. Phys. Soc. Jpn. **54**, 4530 (1985).

[6] A. V. Chubukov and D. I. Golosov, J. Phys.: Condens. Matter **3**, 69 (1991).

[7] L. Seabra, T. Momoi, P. Sindzingre, and N. Shannon, Phys. Rev. B **84**, 214418 (2011).

[8] T. Inami, Y. Ajiro, and T. Goto, J. Phys. Soc. Jpn. **65**, 2374 (1996).

[9] A. I. Smirnov, H. Yashiro, S. Kimura, M. Hagiwara, Y. Narumi, K. Kindo, A. Kikkawa, K. Katsumata, A. Y. Shapiro, and L. N. Demianets, Phys. Rev. B **75**, 134412 (2007).

[10] T. Sakai and H. Nakano, Phys. Rev. B **83**, 100405 (2011).

[11] T. Coletta, T. A. Tóth, K. Penc, and F. Mila, Phys. Rev. B **94**, 075136 (2016).

[12] C. L. Henley, Phys. Rev. Lett. **62**, 2056 (1989).

[13] H. Tanaka, T. Ono, H. A. Katori, H. Mitamura, F. Ishikawa, and T. Goto, Prog. Theor. Phys. Suppl. **145**, 101 (2002).

[14] T. Ono, H. Tanaka, H. A. Katori, F. Ishikawa, H. Mitamura, and T. Goto, Phys. Rev. B **67**, 104431 (2003).

[15] T. Ono, H. Tanaka, O. Kolomiyets, H. Mitamura, T. Goto, K. Nakajima, A. Oosawa, Y. Koike, K. Kakurai, J. Klenke, P. Smeibidle, and M. Meißner, J. Phys.: Condens. Matter **16**, S773 (2004).

[16] Y. Shirata, H. Tanaka, A. Matsuo, and K. Kindo, Phys. Rev. Lett. **108**, 057205 (2012).

[17] T. Susuki, N. Kurita, T. Tanaka, H. Nojiri, A. Matsuo, K. Kindo, and H. Tanaka, Phys. Rev. Lett. **110**, 267201 (2013).

[18] N. Achiwa, J. Phys. Soc. Jpn. **27**, 561 (1969).

[19] H. Nojiri, Y. Tokunaga, and M. Motokawa, J. Phys. Colloques **49**, C8 (1988).

[20] T. Nikuni and H. Shiba, J. Phys. Soc. Jpn. **62**, 3268 (1993).

[21] A. F. Wells, J. Chem. Soc. , 1662 (1947).

[22] A. W. Schlueter, R. A. Jacobson, and R. E. Rundle, Inorg. Chem. **5**, 277 (1966).

[23] Y. Tazuke, H. Tanaka, K. Iio, and K. Nagata, J. Phys. Soc. Jpn. **50**, 3919 (1981).

[24] H. Tanaka, U. Schotte, and K. D. Schotte, J. Phys. Soc. Jpn. **61**, 1344 (1992).

[25] M. Mekata, Y. Ajiro, T. Sugino, A. Oohara, K. Ohara, S. Yasuda, Y. Oohara, and H. Yoshizawa, J. Magn. Magn. Matter **140**, 1987 (1995).

[26] K. Adachi, N. Achiwa, and M. Mekata, J. Phys. Soc. Jpn. **49**, 545 (1980).

[27] H. B. Weber, T. Werner, J. Wosnitza, H. v. Löhneysen, and U. Schotte, Phys. Rev. B **54**, 15924 (1996).

[28] Y. Kousaka, H. Ohsumi, T. Komesu, T. Arima, M. Takata, S. Sakai, M. Akita, K. Inoue, T. Yokobori, Y. Nakao, E. Kaya, and J. Akimitsu, J. Phys. Soc. Jpn. **78**, 123601 (2009).

[29] M. Mino, K. Ubukata, T. Bokui, M. Arai, H. Tanaka, and M. Motokawa, Physica B: Condens. Matter **201**, 213 (1994).

[30] S. A. Zvyagin, D. Graf, T. Sakurai, S. Kimura, H. Nojiri, J. Wosnitza, H. Ohta, T. Ono, and H. Tanaka, Nat. Commun. **10**, 1064 (2019).

[31] A. Sera, Y. Kousaka, J. Akimitsu, M. Sera, and K. Inoue, Phys. Rev. B **96**, 014419 (2017).

[32] M. Hosoi, H. Matsuura, and M. Ogata, J. Phys. Soc. Jpn. **87**, 075001 (2018).

[33] D. Yamamoto, T. Sakurai, R. Okuto, S. Okubo, H. Ohta, H. Tanaka, and Y. Uwatoko, Nat. Commun. **12**, 4263 (2021).

[34] M. M. Altarawneh, C. H. Mielke, and J. S. Brooks, Rev. Sci. Instrum. **80**, 066104 (2009).

[35] S. Ghannadzadeh, M. Coak, I. Franke, P. A. Goddard, J. Singleton, and J. L. Manson, Rev. Sci. Instrum. **82**, 113902 (2011).

[36] T. F. Smith and C. W. Chu, Phys. Rev. **159**, 353 (1967).

[37] A. G. Christy, R. J. Angel, J. Haines, and S. M. Clark, J. Phys.: Condens. Matter **6**, 3125 (1994).

[38] K. Katsumata, K. Sugiyama, and M. Date, J. Phys. Soc. Jpn. **52**, 3312 (1983).